Accretion bursts in high-mass young stellar objects

Alessio Caratti o Garatti[1,2], Bringfried Stecklum[3], Verena Wolf[3]

[1]INAF-Osservatorio Astronomico di Capodimonte, [2]Dublin Institute for Advanced Studies, [3]Thüringer Landessternwarte Tautenburg

Introduction: In the past few years, accretion bursts in young stellar objects (YSOs) have gained increasing relevance in star formation. The latest picture of YSO evolution suggests that a large portion (up to 30-40%) of their final mass might be gathered during accretion bursts (e.g., [1,2]). Indeed, most recent observations have corroborated the idea that episodic accretion is a universal phenomenon across mass and time in star formation. The study of episodic accretion in high-mass young stellar objects (HMYSOs) is still in its infancy. In the past six years, we have been detecting four bona-fide bursts from HMYSOs (S255IR NIRS3, NGC 6334I-MM1, G358.93-0.03 MM1, G323.46-0.08; e.g., [3,4,5,6]), two (M17 MIR, V723 Car; [7,8]) from possible HMYSOs in the making, and two periodic HMYSOs outbursters (G24.33+0.14, G107.30+5.64; [9]).
Despite the small sample of outbursters, a large variety of physical properties (in terms of accreted mass, released energy and length of the burst) has been observed, similarly to their low-mass counterparts. However, released energy, mass accretion rates and accreted mass of such episodes are orders of magnitude larger than in low-mass young stars.
In addition to "classical" direct methods for detecting bursts, such as multi-wavelength light-curves and multi-epoch spectroscopy, other indirect tracers, like CH_3OH and H_2O maser flares or radio jet bursts, can be used for revealing and studying episodic accretion in HMYSOs.

MAIN PARAMETERS OF KNOWN ACCRETION BURSTS FROM HMYSOs

NAME	M_*	L_{pre}	L_{burst}	Rise time	Δt	Rel. En.	$\dot{M}_{acc}^{burst}$	M_{acc}	Detection	Tracers	Ref.
	($M_\odot$)	($L_\odot$)	($L_\odot$)	(yr)	(yr)	(J)	($M_\odot$/yr)	(M_{Jup})	wavelength range		
S255IR NIRS3	20	3×10^4	1.6×10^5	0.4	2.5	1.2×10^{39}	5×10^{-3}	2	NIR-mm (K~8.5 mag)	NIR spectra, SED, CH_3OH & H_2O maser + radio jet flares	3,10,11
NGC 6334I MM1†	6.7	3×10^3	4.9×10^4	0.6	>6	3.2×10^{39}	10^{-3}	>0.3	MIR-mm (K>21 mag)	SED, CH_3OH & H_2O maser flares	4,12
G358.93-0.03 MM1††	9.7	7.6×10^3	1.9×10^4	0.2	0.75	2.9×10^{38}	1.8×10^{-3}	0.6	MIR-FIR	SED, CH_3OH & H_2O maser flares	5,13
G323.46–0.08	13	10^5	2.5×10^5	~3	~7.6	2.3×10^{40}	2.8×10^{-3}	23	NIR-MIR (K~5.5 mag)	SED, CH_3OH maser flare	6,14
M17 MIR	5.4	1.4×10^3	9×10^3	-	9-20	-	$\sim2\times10^{-3}$	-	MIR-FIR (K>22 mag)	SED, H_2O maser flare	7
V723 Car	10?	$\sim4\times10^3$	-	4	~15	-	-	-	NIR-FIR (K~12.9 mag)	NIR spectra, SED	8

† Ongoing burst; †† FIR afterglow still active

NIR SPECTRA: EVOLUTION OF THE S255IR NIRS3 BURST

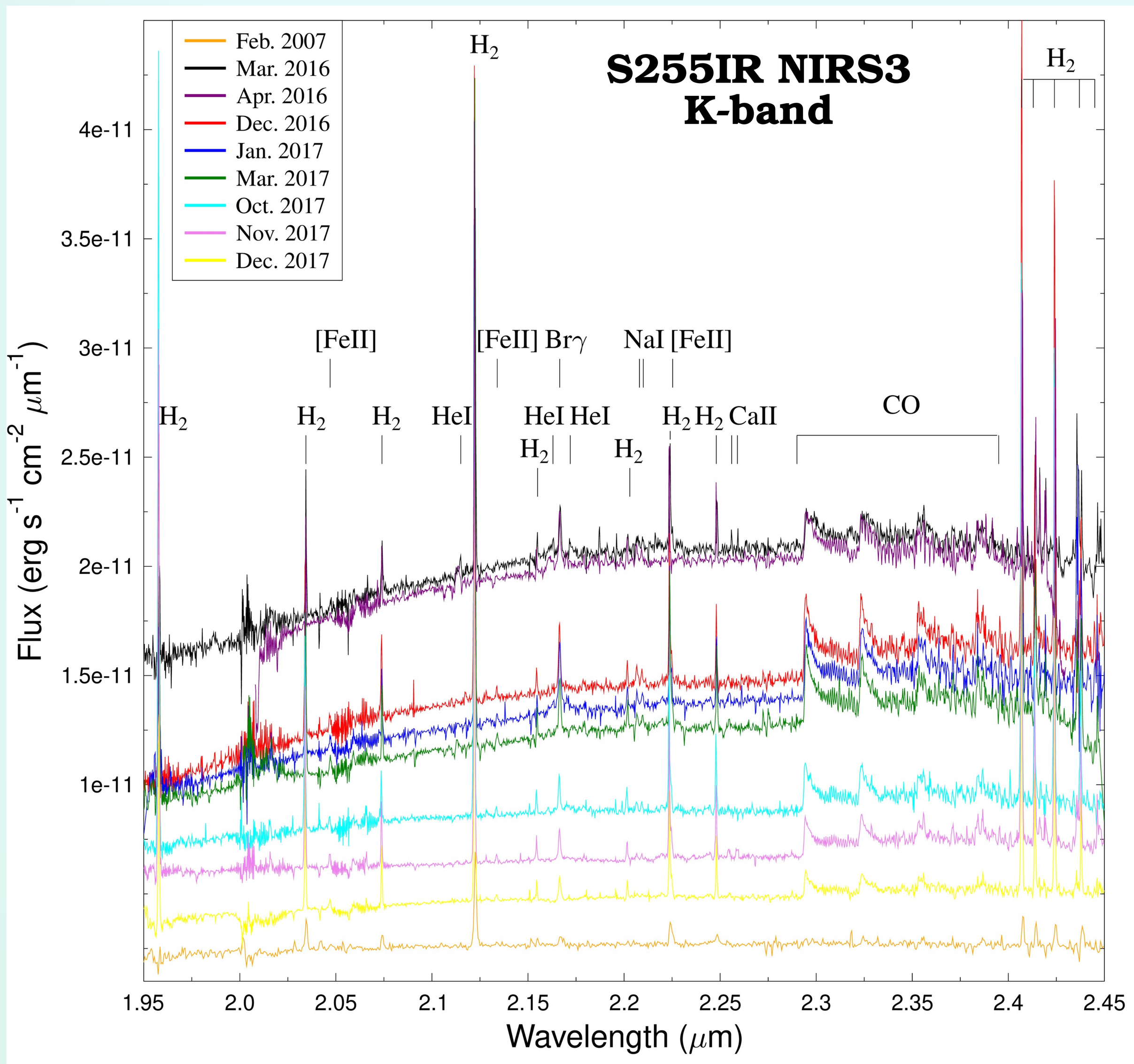

Figure 1: Pre-outburst (orange, Feb. 2007) and outburst multi-epoch K-band spectroscopy of the red-shifted outflow cavity of S255IR NIRS3 (adapted from [3]). The cavity acts as a mirror allowing to detect both continuum and line emission from the inner disk. The pre-outburst spectrum only shows H_2 lines in emission, whereas the burst spectra display lines typical of EXor-type bursts in low-mass YSOs. The first-epoch burst spectrum (black, March 2016) presents data ~1 month after the peak of the event. It shows: CO bandheads, NaI, and CaII lines originating from the disk; HeI and HI lines emitted closer to the central source and tracing accretion onto the star and/or disk winds. An increase of fluxes from shocked H_2 lines is detected at all epochs, peaking ~13 months after the maximum. Notably, the K-band spectrum of V723 Car also shows H_2 and Brγ lines, and CO bandheads in emission (see [8]).

SEDs: NIR VISIBLE vs NIR DARK ACCRETION BURSTS

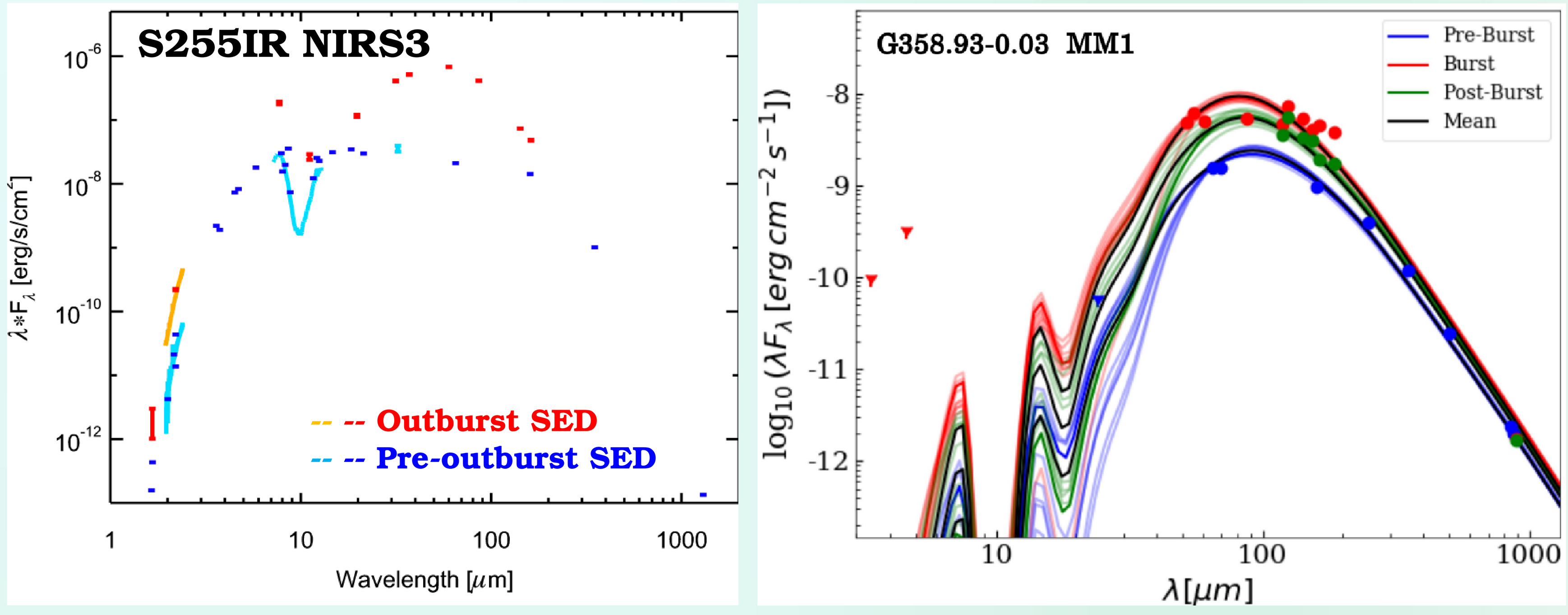

Figure 2. Left: Pre- (cyan and blue) and outburst (orange and red) spectral energy distributions (SEDs) of S255IR NIRS 3 (adapted from [3]). Dark colours indicate photometric measurements and light colours denote spectra. The HMYSO (A_V~40 mag; age~10^4 yr) is detected in the NIR. **Right:** G358 MM1 burst. Modelled (continuos line) and observed (circles and triangles) pre-burst SEDs (blue), together with its burst (red) and post-burst (afterglow) SED (green). Triangles mark upper limits. Weighted mean-models are shown in black (adapted from [13]). As a consequence of the mild-burst, the SEDs show variations from the MIR to FIR regime but not in the millimetric. The massive protostar is extremely young (a few 10^3 yr) and extincted (A_V>100 mag), the burst is undetected in the NIR. An "afterglow" at FIR wavelengths is still present after the burst is over.
The variety in the SEDs of the sampled massive bursters indicates that accretion bursts of different strength and duration occur at different stages of massive star formation.

OTHER TRACERS OF ACCRETION BURSTS IN HMYSOs: CH_3OH & H_2O MASER FLARES, RADIO JET BURST

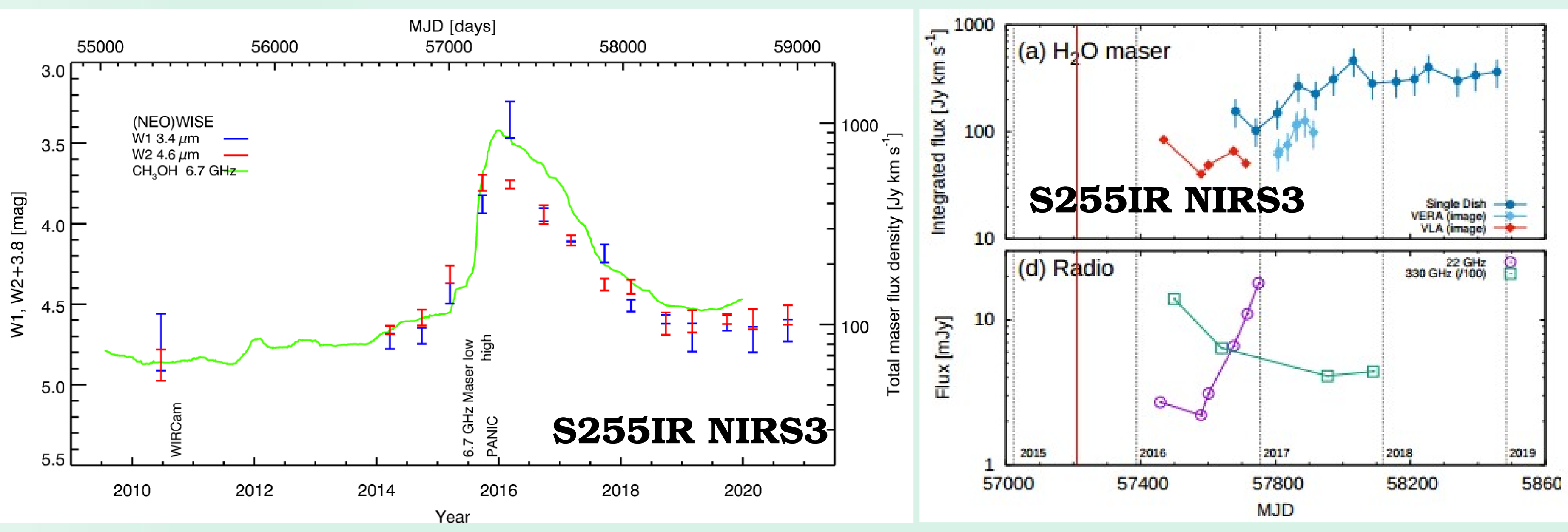

Figure 3. Left: S255IR NIRS3 burst evolution. The total power of the 6.7 GHz CH_3OH maser light-curve (green) matches those from NEOWISE (W2 magnitudes in red were shifted by 3.8 to match the W1 light-curve in blue) (adapted from [16]). Notably, all the four bona-fide bursts displayed 6.7 GHz CH_3OH maser flares, that actually triggered the discoveries. As MIR radiation from heated dust is the pumping mechanism of this maser transition, 6.7 GHz methanol maser flares are the perfect beacon for signaling accretion bursts in HMYSOs.
Right: As accretion turns into ejection, the free-free emission from the radio jet is bursting (bottom right, purple) while the dust continuum (green) returns to the pre-burst level. In S255IR NIRS3 this happens ~13 months after the beginning of the burst (red line). Also the H_2O masers at 22 GHz flared-up (upper right), suggesting a similar origin as for the radio jet burst and the H_2 emission, possibly a wind (figures adapted from [17]).

BURST INDUCED SEDs CHANGES: FROM STATIC TO TIME-DEPENDENT MODELLING

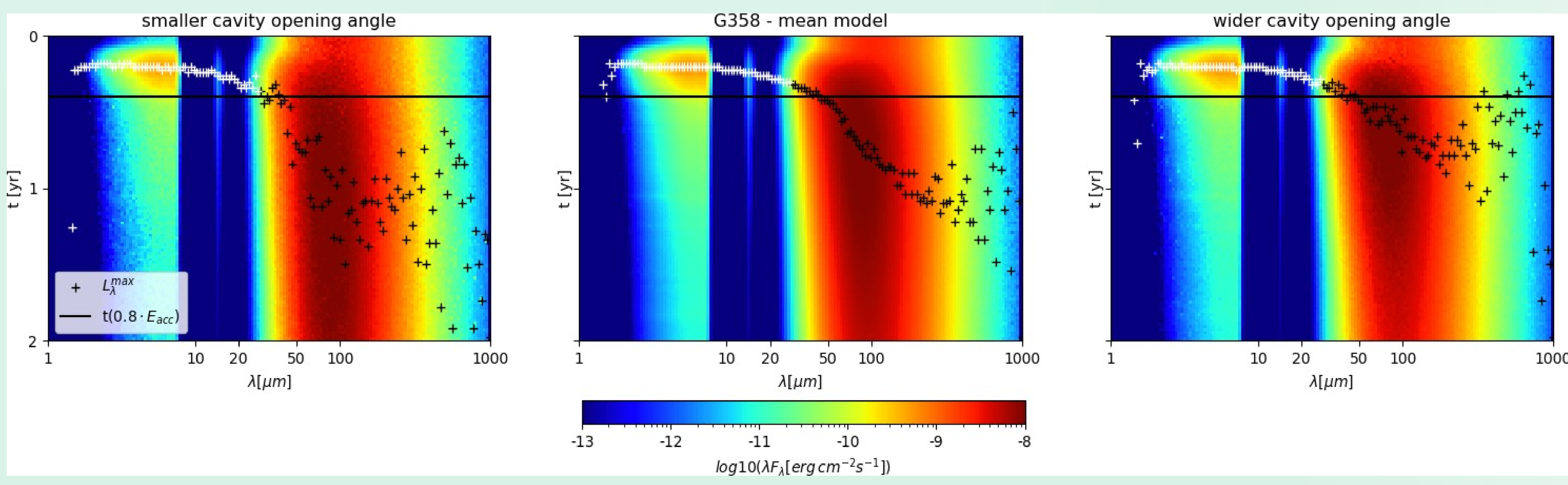

Figure 4. SED time-dependent radiative transfer (RT) modeling of the G358 MM1 burst (from [14]), based on TORUS [18] simulations. Plots also show the influence of the outflow cavity opening angle on heating and cooling the disk/envelope. The **middle plot** displays the dynamic spectrum of our mean model (see Fig. 2, right panel, black curves), assuming a temporal change of the accretion rate, which resembles the CH_3OH maser light-curve, and a burst energy release as derived from our static modelling. **Left** and **right** plots are the same, but for cavity opening angles of 75% (left) and twice the value (right) of the mean model. Black/white crosses indicate the peak flux timing at each wavelength. The black line marks the time when 80% of the total burst energy has been released. Cooling and heating timescales depend on wavelength and density of the circumstellar environment. The wider the cavity opening angle, the faster the energy escapes the system. Including the time domain in RT modelling will help to better constrain both burst and system characteristics. The scatter at longer wavelengths is due to numerical noise in the Monte Carlo simulation.

Conclusions

Accretion bursts are a common feature also in massive protostars, at different stages of their evolution. ΔL_{bol} and $\Delta\dot{M}_{acc}$ values so far observed increase by an order of magnitude during such episodes, suggesting that relatively mild bursts have been detected. This idea is also supported by the relatively short length of such bursts, from some months to several years (although the NGC 6334I MM1 burst is still active). The observed accretion bursts are typically accompanied by ejection bursts or increased wind/outflow activity, traced by an increase in flux of the H_2 emission lines, and/or by radio jet and H_2O maser flares. Finally, we are constructing time-dependent RT models with TORUS to match the observed SED time-variations and study how accretion bursts affect the protostellar environment. These RT models point at the presence of thermal afterglows well after the burst has ceased.

References: [1] Fischer et al. 2019, ApJ, 872,183; [2] Meyer et al. 2021, MNRAS, 500, 4448; [3] Caratti o Garatti et al. 2017, Nature Phys., 13, 276; [4] Hunter et al. 2017, ApJL ,837, 29; [5] Brogan et al. 2019, ApJL, 881, 39; [6] Proven-Adzri et al. 2019, MNRAS, 487, 2407; [7] Tapia et al. 2015, MNRAS, 446, 4088; [8] Chen et al. 2021, ApJ in press, arXiv:2108.12554; [9] Stecklum et al. in prep.; [10] Moscadelli et al. 2017, A&A, 600, L8; [11] Cesaroni et al. 2018, A&A, 612, A103; [12] Hunter et al. 2021, ApJL,912, 17; [13] Stecklum et al. 2021, A&A, 646, A161; [14] Wolf et al. in prep.; [15] Caratti o Garatti et al. in prep.; [16] Stecklum et al. 2018, "Watching a Massive Star Grow", online procedings; [17] Hirota et al. 2021, A&A, 647, A23; [18] Harris et al.2019, Ast. & Comp., 27, 63